

SOME ELECTROCHEMICAL PROPERTIES OF RANEY NICKEL

Olga MARHOLOVÁ^a, Karel SMRČEK^a, Zdeněk MINISTR^a and Zdeněk SPITZER^b^a ČKD, Semiconductor Department, Prague 4 and^b Institute for Research and Exploitation of Fuels, 250 97 Běchovice

Received June 23rd, 1981

The connexion between the functioning of the Raney nickel catalyst in a hydrogen anode and the conditions of its preparation (mode of grinding the alloy, deactivation, and storage of the catalyst) was investigated. The relation between the internal surface area and the activity of the catalyst is discussed.

Raney nickel has been used for many years as catalyst in anodes of alkaline hydrogen-oxygen fuel cells. Its chemical, electrochemical, structural, and other properties have been studied by many authors^{1,2}. It has been used mainly in hydrophilic diffusion electrodes either of the sintered¹ or supported type^{3,4}, and exceptionally also in semihydrophobic electrodes operating without overpressure⁵.

Recently, we turned our attention to this catalyst as a substitute for platinum in semihydrophobic anodes. The problems to be solved were related to the preparation and deactivation of fine powdered fractions for the preparation of the operating layer.

The surface area of the nickel catalyst plays a significant role in functioning of the gas electrode; it can be assumed that the maximum obtainable current is proportional to the product of the catalytically active surface area and exchange current density. It was indeed observed⁶ that the latter has on different nickel catalysts (metallurgical, electrolytic, and Raney Ni) practically the same value, namely $(1.5 \pm 0.7) \cdot 10^{-6}$ A/cm².

A larger surface can be made available also by decreasing the particle dimensions; smaller catalyst particles are generally preferable for the functioning of semihydrophobic electrodes. However, disintegration of the catalyst particles brings about some unfavourable changes of the freshly formed surface by interaction with the medium. A similar phenomenon takes place during deactivation of an active catalyst.

The Raney nickel catalyst is obtained by leaching out aluminum from a finely ground Ni-Al alloy (about 1 : 1 by weight). The remaining nickel has a highly disordered structure with a large inner surface area and a high catalytic activity for ionization of hydrogen in alkaline medium. Its surface is covered with adsorbed hydrogen, which is the cause of the pyroforicity of this catalyst. The atomic ratio of adsorbed hydrogen to nickel is according to different authors^{2,7-10} in the range 0.1–2.6.

To facilitate handling of the catalyst, it must be transformed from its active form to an inactivated one, provided with an oxide layer, which can be removed by the action of hydrogen in alkaline medium leading to reactivation. The controlled oxidation is achieved either electrochemically^{1,11-13} or by the action of air or oxygen^{11,14-16} or other oxidants¹³.

To judge the quality of the nickel catalyst, its electrochemical properties are of basic importance. Our aim was to elucidate the connexion between these pro-

erties and the treatment of the catalyst by different technologies, grinding, and deactivation.

EXPERIMENTAL

Ni-Al Alloys and their Grinding

We used four Ni-Al alloys differing by their composition and particle size (Table I). The particle size of the catalysts after leaching was the same as that of the nonleached alloy.⁷

To study the influence of grinding, the starting alloy was first disintegrated, ground, and fractionated to obtain a fraction below 0.1 mm, which was further ground open to the air, in water, and in ethanol. This was done in a drum of 15 l holding capacity containing 7 kg of balls and 7 kg of grist, eventually 5 l of water or ethanol. The duration of grinding was 48 h. The speed

TABLE I

Fractions of powdered alloys and catalysts prepared therefrom

Symbol	Alloy fraction				Catalyst				
	particle size, μm	Ni, %	Al, %	Ti, %	active state	inactive state	Ni, %	Al, %	Ti, %
F 11	2-6	35.8	45.4	—	—	60	87.6	—	—
F 21 ^a	2-6	31.5	27.8	—	—	62	72.1	2.3	—
F 31 ^b	2-6	38.9	49.8	—	—	64	63.1	8.8	—
G 11	6-36	43.6	53.0	—	—	87	76.3	4.6	—
G 21 ^a	6-36	26.3	28.7	—	—	82	60.3	13.3	—
G 21 ^b	6-36	42.0	53.0	—	—	98	67.1	—	—
103	6-45	50.8	46.3	2.9	—	110-114 ^a	—	—	—
103	6-45	50.8	46.3	2.9	—	103	76.7	4.0	2.5
104	6-45	54.6	45.5	—	—	104 ^a	73.9	5.0	—
105	6-45	53.8	45.9	—	—	105 ^c	78.4	3.8	—
106	2-6	52.7	44.9	2.6	—	106	85.0	2.0	2.4
62	2-6	31.5	27.8	—	121	122	72.1	2.3	—
83	6-36	54.0	46.6	2.5	123	124	70.0	12.8	2.4
99	6-45	51.4	49.3	—	115	116	76.3	3.7	—
100	0-36	53.3	46.6	—	125	126	83.2	1.9	—
103	6-45	50.8	46.3	2.9	117	118	77.5	4.0	2.5
106	2-6	52.7	44.9	2.6	119	120	85.0	2.0	2.4
104	6-45	54.6	45.5	—	—	104 ^a	73.9	5.0	—
8	0-40	42.5	52.5	—	—	1	78.3	2.1	—
8	0-40	42.5	52.5	2.6	—	2	79.1	2.5	—

^a Ground under water, ^b under ethanol; otherwise on the air.

of rotation (55 r.p. min) was chosen so that the balls were set in a vertical oscillatory motion. The ground alloy was dried and fractionated on a Walther fractionating apparatus to obtain a coarse (G) and a fine fraction (F).

Measurement of the Rate of Leaching

The rate of leaching of the alloys can be easily evaluated from the quantity of evolved hydrogen. A simple glass apparatus was used and the experimental conditions were kept constant (quantity of the alloy, stirring, initial temperature of the solutions). A weighed amount of the alloy (about 0.5 g) was put into a glass bottle with three necks provided with a magnetic stirrer and a thermometer. A chosen quantity of 2.5M-KOH was quickly added and the volume of the formed gas was measured by a gas burette. The volume as a function of time gave the rate of the gas evolution. The volume was corrected for normal temperature and pressure.

Preparation of the Catalysts

Samples of nickel catalysts were prepared by a three-stage leaching of the ground alloy in 5M-KOH at 90–100°C, the reaction mixture was neutralized with a 10% tartaric acid solution and washed with distilled water. Deactivation was done by 3% H₂O₂. The deactivated catalysts were dried on the air and care was taken in order that the temperature did not exceed 30°C. The product was stored in glass bottles with ground glass stoppers. Tests were made immediately after preparation and at intervals to follow the ageing (for up to 15 months). To determine the influence of deactivation, two samples were prepared from each charge (Table I), the first of which was taken away before deactivation and was stored under ethanol, and the second one was deactivated and was stored in the dry state.

Measurement of the Catalyst Properties

The specific surface area was measured by the BET method on a conventional glass apparatus; the samples were degasified in a sorption cell joined with the apparatus first at the room temperature and then 4 h at 180°C. Argon was used rather than nitrogen since the latter would interact with the nickel surface, especially with the active samples. In some cases, the method of thermal desorption of nitrogen using an apparatus modified according to Grubner was employed; in this case the samples were dried for 4 h at 150°C in vacuum prior to measurement. Microphotographs of the powdered samples were made on a JEOL JSM-T20 scanning microscope.

Preparation of Electrodes and Electrochemical Measurements

Laboratory electrodes were prepared by rolling a mixture of deactivated catalyst with 2 percent of PTFE dispersion GP₁ (ICI, Great Britain) wetted with ethanol and kneaded for 15 min. The layer thickness was 1 mm and the square density was 138–308 mg/cm². Electrochemical measurements were done with disc-shaped electrodes of 10 cm² functional area in a half-cell arrangement in 7M-KOH at 80 ± 2°C. The electrodes were mounted in special pressure vessels and at an overpressure of hydrogen 0.0608 MPa; the reference electrode was Hg/HgO in the same solution. The electrodes were activated with hydrogen for 24 h at 80°C. After recording the polarization curve, for H₂ content determination the electrode was loaded with a constant current density of 30 mA/cm² until a potential of -0.4 V was reached.

TABLE II
Influence of grinding conditions

Sym- bol	Alloy fraction				Catalyst			
	particle size, μm	grinding medium	H_2 ml min^{-1}	yield %	symbol	square density g/cm^2	α A g^{-1}	R_s Ωcm^2
F 11	2— 6	air	200	6	60	0.1903	0.301	2.11
F 21	2— 6	water	25	42	62	0.1433	0.224	3.60
F 31	2— 6	ethanol	195	60	64	0.1865	0.343	1.88
G 11	6—36	air	85	10	87	0.1967	0.710	0.87
G 21	6—36	water	30	50	82	0.2022	0.198	3.00
G 31	6—36	ethanol	140	35	98	0.2135	0.722	0.79

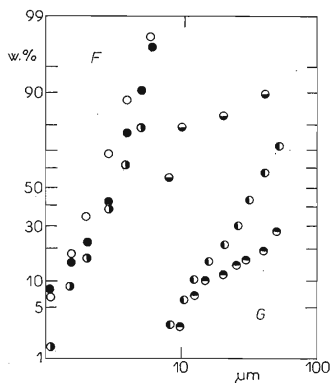


FIG. 1

Particle size distribution for fractions F and G of powdered Ni-Al alloy. \circ \bullet ground in the presence of air, \circ \bullet ground under water, \circ \bullet ground under ethanol

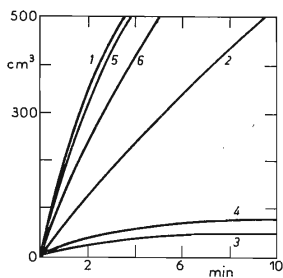


FIG. 2

Rate of hydrogen evolution during leaching of Ni-Al alloy ground in the presence of air (1 fraction F, 2 fraction G), under water (3 F, 4 G), or under ethanol (5 F, 6 G)

RESULTS AND DISCUSSION

The electrochemical activity of the Raney nickel catalyst depends mainly on the state of its surface and on its magnitude; on the other hand the catalyst activity influences the electrode performance. Generally, the surface of powdered materials depends on the particle size and can be increased by grinding. Grinding of metals in the presence of the air can lead to oxidation of their surface, which in the case of the nickel catalyst is undesirable. Grinding in a protecting medium is hence preferable.

For comparison and verifying the above deductions, the alloy was ground in three different media, air, water, and ethanol. The products were fractionated to a fine (F) and coarse fraction (G) (Table II). Their particle size distributions are shown in Fig. 1. It is seen that the grinding in ethanol is more effective than in water and this in turn is more effective than in the dry state. The composition of the fractions is given in Table I, from which it is seen that the products ground in water have a low content of the metals, apparently as a result of the formation of hydrated oxides by a reaction with water during grinding. The chemical composition of the products ground in ethanol and in the dry state, however, is not appreciably different. There is a small difference in the composition of the fine fraction suggesting that corrosion proceeds during grinding in the dry state more strongly than in ethanol.

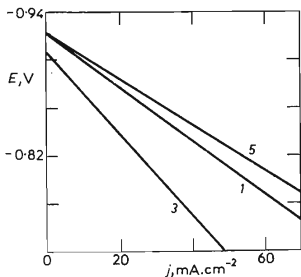


FIG. 6

Polarization curves for catalyst fraction F.
1 Catalyst No 60, 3 62, 5 64 (Table II)

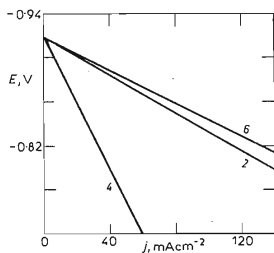


FIG. 7

Polarization curves for catalyst fraction G.
2 Catalyst 87, 4 82, 6 98 (Table II)

As seen from Fig. 2, the alloy ground under water shows a slow course of leaching as a result of its blocked surface and an accumulation of nonleachable components by corrosion during grinding. These differences are well illustrated by photographs of the particles in the range 6–36 μm (Figs 3–5*): the particles ground under water are strongly corroded, whereas the other show clear contours with a relatively intact surface.

Differences in electrochemical properties of differently ground catalysts are illustrated by Figs 6 and 7 and Table II. The tests were made with electrodes of the supported type, which do not affect the structure and surface of the tested catalyst. Both fractions were measured, although the fine one did not prove well in the overpressure electrodes, apparently because of a slow transport of the reacting gas. The electrochemical activity of the Raney nickel prepared by grinding under water was worst. Differences between the other two methods of grinding are not too significant, however grinding in ethanol seems to be preferable with respect to the consumption of energy and electrochemical properties.

The specific surface area of the nickel catalyst is not altered by grinding of alloy, since it is given by the finely porous structure of the catalyst grains. The specific surface area determined by electrochemical desorption of hydrogen was 48.93 m^2/g for ten samples of particle size up to 6 μm and 48.85 m^2/g for 24 samples of particle size up to 40 μm , *i.e.*, practically the same. However, the particle size of the catalyst can play a role in optimizing the structure of porous electrodes prepared therefrom.

The deactivated form of the catalyst was prepared at different times of deactivation (compare Experimental) with results given in Table III. Increasing time of deactivation enhances the formation of the passivating surface layer, which is stabilized after some time. It turned out that 5 min of deactivation is sufficient.

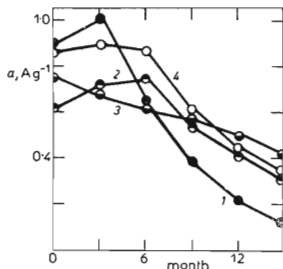


FIG. 8

Dependence of Ni catalyst performance on time of storage. 1 Catalyst 106, 2 104a, 3 105c, 4 103 (Table I)

* See insert facing p. 1696.

In Fig. 8 is shown the influence of ageing on the activity of the catalyst. It is apparent that the catalysts can be stored for up to 6 months without affecting their quality, but afterwards their activity drops gradually, probably as a result of structural changes of the oxide surface layers.

TABLE III
Electrochemical parameters after different times of deactivation with hydrogen peroxide

Deactiv. time min	Catalyst	α $A\ g^{-1}$	R_s $\Omega\ cm^2$
0	110	1.17	0.32
5	111	1.06	0.58
10	112	0.72	0.80
15	113	0.73	0.90
30	114	0.71	0.80
2×30	114a	0.83	0.84

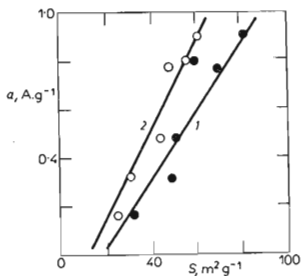


FIG. 13

Dependence of performance of catalysts on their specific surface area. The latter was determined 1 by the BET method, 2 by electrochemical desorption of hydrogen (Table IV)

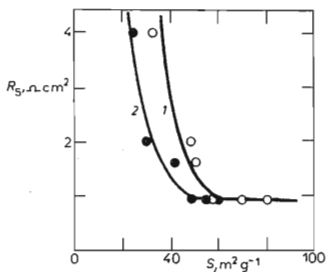


FIG. 14

Dependence of polarization resistance on specific area of catalysts. The latter was determined 1 by the BET method, 2 by electrochemical desorption of hydrogen (Table IV)

TABLE IV
Electrochemical parameters and specific surface area measured by different methods

Catalyst	Sq. dens. g/cm ²	α A g ⁻¹	R_s Ω cm ²	Specific surface area, m ² /g			
				el. des. of H ₂	BET inactive state	BET active state	therm. des. of N ₂ in inact. state
115	—	—	—	—	—	69.9	—
116	0.186	0.777	0.94	48.1	20.7	—	47.3
117	—	—	—	—	—	81.1	—
118	0.157	0.867	0.91	60.5	3.3	—	26.0
119	—	—	—	—	—	56.7	—
120	0.206	0.805	0.96	55.2	4.0	—	—
121	—	—	—	—	—	31.5	—
122	0.138	0.163	4.0	25.0	—	—	25.3
123	—	—	—	—	—	48.8	—
124	0.175	0.317	2.0	29.9	—	—	41.3
125	—	—	—	—	—	49.9	—
126	0.171	0.480	1.62	43.4	—	—	26.2
104a ^a	0.169	0.887	0.87	43.9	39.3	59.6	28.3
1 ^b	0.234	0.461	1.03	68.1	1.07	106.0	—
2 ^b	0.308	0.428	0.99	50.9	0.52	90.4	—

^a Activated with hydrogen in 7M-KOH at 70°C, ^b reduced by heating in hydrogen atmosphere for 17 h at 350°C.

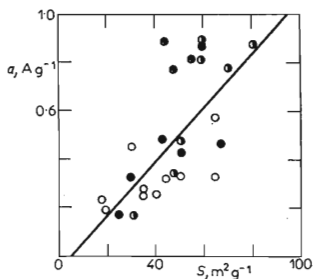


FIG. 15
Dependence of catalyst performance on specific surface area for a series of Ni catalysts. ● supported electrodes, surface area from electrochemical desorption of hydrogen, ◐ supported electrodes, surface area from BET measurements ○ sintered electrodes, surface area from BET measurements¹⁹

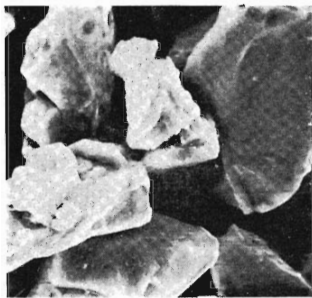


FIG. 3
Surface of Ni-Al alloy, fraction G (6–36 μm) ground in the presence of air. Magnification 3 500×

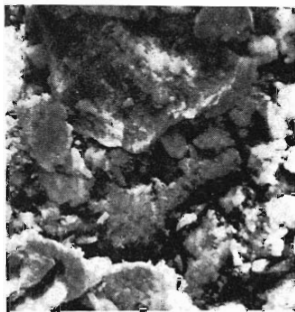


FIG. 4
Surface of Ni-Al alloy, fraction G (6–36 μm) ground under water. Magnification 3 500×

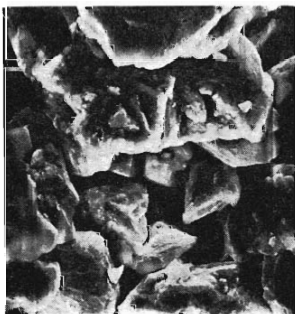


FIG. 5
Surface of Ni-Al alloy, fraction G (6–36 μm) ground under ethanol. Magnification 3 500×

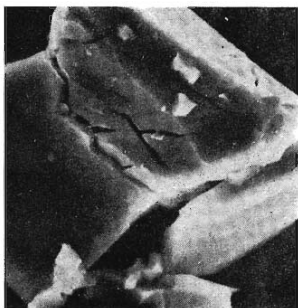


Fig. 9
Surface of Ni catalyst before inactivation, stored under ethanol and not dried. Magnification 3 000 \times



FIG. 10
Surface of Ni catalyst inactivated by hydrogen peroxide and dried on the air. Magnification 3000 \times



FIG. 11
Surface of Ni catalyst dried on the air at controlled temperature. Magnification 3 000 \times



FIG. 12
Surface of Ni catalyst oxidised pyroforically by air. Magnification 3 000 \times

The mentioned dependences give some information about the surface state of the catalytic particles. Measurements of the specific surface area revealed differences between the active and inactive states (Table IV). This is in agreement with the assumption that the surface oxide layer seals more or less the inner pore surface of the catalyst, which is free in the active samples. This surface can be freed also by reduction of the inactive catalyst with hydrogen at elevated temperatures, or during activation with hydrogen in an electrolyte solution. The true active surface area should be equal to that determined by electrochemical desorption of hydrogen on the catalyst activated in an electrolyte solution (Table IV). However, the latter quantity was usually smaller than the surface area determined by the BET method, an evidence that a fraction of the total surface is inaccessible for the electrochemical process.

Observations with the scanning electron microscope are rather inconclusive. In Fig. 9* is shown the surface of active particles stored under ethanol, which appears identical with the surface of particles deactivated by hydrogen peroxide, Fig. 10*, or with particles dried on the air at a temperature below 50°C, Fig. 11*. Visible changes are observable with a catalyst that was spontaneously (pyrophorically) oxidised (Fig. 12*). The highly developed surface area is obviously due to submicroscopic pores; cracks visible in the photographs have their origin in grinding of the alloy.

The electrochemical performance of the catalysts, α , expressed in A/g, shows a correlation with the specific surface area, S , according to expectation (Fig. 13). A similar dependence was found for the activity with respect to hydrogenation of oils¹⁷.

The dependence of the polarization resistance, R_p , on the specific surface area has an exponential character (Fig. 14) as found earlier in similar cases^{4,18}.

To obtain a more reliable dependence of α on S , we summarized all our measurements including the previously published ones^{4,10}, which were done with sintered electrodes. The latter can be included in the given ensemble since it was found experimentally¹⁹ that pressing and heating does not cause a marked change of the specific surface area of the Raney nickel. Regression analysis gave the linear dependence $\alpha = 0.0114 S - 0.0423$, which passes close to the origin of coordinates, thus approaching the theoretical expectation (Fig. 15).

REFERENCES

1. Justi E., Winsel A.: *Kalte Verbrennung*. Steiner, Wiesbaden 1962.
2. Fasman A. B., Sokolskii D. V.: *Struktura i Fizikokhimicheskie Svoistva Skeletnykh Katalizatorov*. Nauka, Alma-Ata 1968.
3. Sturm F. v.: *Siemens-Z.* 39, 453 (1965).
4. Smrček K., Ministr Z.: *Metalloberfläche* 25, 195 (1971).
5. Parmentier C., Blanchart A., Brandt C., Vandenborre H., Spaepen G.: 4th Int. Symposium on Fuel Cells, Antwerp 1972.

* See insert facing p. 1696.

6. Abramzon O. S., Chernyshov S. F., Pshenichnikov A. G.: *Elektrokhimiya* **12**, 1667 (1976).
7. Dousek F. P., Jansta J., Řiha J.: *This Journal* **31**, 4252 (1966).
8. Dousek F. P.: *Thesis*. Czechoslovak Academy of Sciences, Prague 1964.
9. Sturm F. v., Richter G.: *Electrochim. Acta* **10**, 1169 (1965).
10. Smrček K., Jandera J.: *This Journal* **39**, 1899 (1973).
11. Döhren H. H. v., Kalberlah A.: *Chem.-Ing.-Tech.* **40**, 176 (1968).
12. Sturm F. v., Cnobloch H., Nischik H., Marchetto M.: *Int. Symp. Brennstoffelemente*, Dresden 1967.
13. Jung M., Döhren H. H. v.: *Aktuelle Batterieforschung*. Varta, Frankfurt/Main 1966.
14. Wendtland R.: *Brennstoff-Chem.* **50**, 59 (1969).
15. Ewe H., Justi E., Schmitt A.: *Energy Conversion* **14**, 35 (1975).
16. Ewe H., Justi E., Selbach H. J.: *Electrochem. Power Sources Int. Symp. ISE*, Varna 1977. Ext. Abstr. No. 61.
17. Coenen J. W. E., Linsen G. B. in the book: *Physical and Chemical Aspects of Absorbents and Catalysts* (B. G. Lindsen, Ed.), p. 508. Academic Press, London 1970.
18. Mund K., Richter G., Sturm F. v.: *J. Electrochem. Soc.* **124**, 1 (1977).
19. Ministr Z., Konopleva N.: Unpublished results.

Translated by K. Micka.